He^{++} Transport in the PDX Tokamak

R. J. Fonck and R. A. Hulse
Plasma Physics Laboratory, Princeton University, Princeton, New Jersey 08544
(Received 9 November 1983)

A powerful new approach to the study of particle transport and helium ash confinement in high-temperature fusion plasmas is demonstrated by charge-exchange recombination spectroscopy of He^{++} in Ohmically heated PDX discharges. Time- and space-resolved measurements of He^{++} density following a short puff of helium gas into the plasma edge are fitted with use of a diffusive/convective transport model with coefficients $D = (2.1 \pm 0.9) \times 10^4$ cm^2 s^{-1} and $v(r)/D = (0.8 \pm 0.3)\partial(\ln n_e)/\partial r$.

PACS numbers: 52.25.Fi, 34.70.-e, 52.55.Gb, 52.70.Kz

The expectation of significant alpha particle densities during D-T operation in the present generation of tokamak experiments (e.g., $n_\alpha \approx 10^{12}$ cm^{-3} at $Q = 1$ in TFTR) has led to discussion of various techniques which will allow radially resolved measurements of both fast (3.5 MeV) and thermalized alphas.[1] Earlier studies of helium pumping or transport relied either on an indirect inference of central helium density via changes in the electron density[2] or on the detection of ^{3}He through nuclear processes.[3] Since ash control devices, such as divertors and pumped limiters, are necessarily located at the edge of a hot plasma, only direct knowledge of the confinement and transport of the thermal He^{++} throughout the plasma allows reasonable modeling of the effects of manipulation of the plasma edge on the central He^{++} concentration.[4]

Helium and other very low-Z impurities are attractive for particle transport studies because they are fully stripped throughout most of the discharge. This greatly simplifies the atomic physics (particularly ionization and recombination) which must be considered in order to arrive at accurate measurements of transport coefficients for these ions.[5] Previously, studies of particle transport in tokamaks have concentrated on heavier impurities which still have electrons and emit line radiation from the hot plasma core.[6-9] Such studies are limited in accuracy by uncertainties in electron temperature and density profiles and imprecise knowledge of atomic rates for high-Z ions.[10]

In this paper, we present the first example of detailed transport coefficient determination for a low-Z impurity by following fully ionized helium through a tokamak plasma after a puff of He was introduced at the plasma edge. The measurements were made in the PDX tokamak using charge-exchange recombination spectroscopy,[11-13] wherein a highly collimated (full width at half maximum ~ 3 cm), low-power (8 kW), diagnostic neutral deuterium beam is injected across the line of sight of a spectrometer. In the intersection volume of the neutral beam and the spectrometer sightline, charge-exchange reactions between the fast D^0 and thermal He^{++} produce He^+ in excited states which decay via photon emission. The He^+ $\Delta n = 2 - 1$ transition at 304 Å is detected for these measurements since the beam energy of 15 keV/u is too low to populate significantly levels with $n > 2$. The 20-ms beam pulse is square-wave modulated to allow discrimination of the beam-induced signal from the background radiation.[14]

The PDX tokamak was run with graphite rail

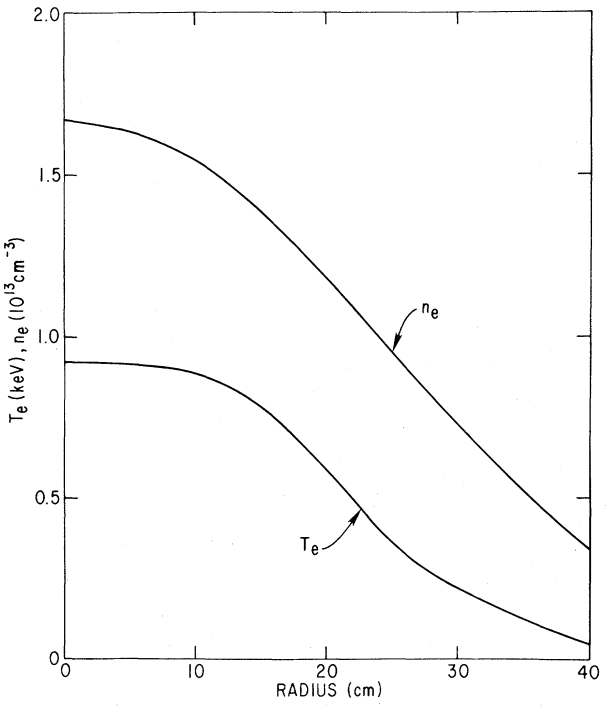

FIG. 1. Electron density and temperature profiles obtained from Thomson scattering at $t = 550$ ms. Experimental uncertainty is 5%–10%.

limiters giving a minor radius of $a = 40$ cm. The Ohmically heated H^+ discharges had major radius $R_{pl} = 150$ cm, $I_{pl} = 270$ kA, $B_T = 13$ kG, and $Z_{eff} = 2.4$. The total discharge pulse length was 900 ms, and a short puff of helium was injected into the plasma at $t = 365$ ms, causing a rise in $\bar{n}_e$ of ~ 8%. Plasma electron density and temperature profiles at $t = 550$ ms are shown in Fig. 1. No discernible magnetohydrodynamic activity was present during the experiment.

The time evolution of the near-central ($r = 7$ cm) He^{++} density and central-chord He^+ 304-Å intensity following the gas pulse are shown in Fig. 2. A sharp rise in $n_{He^{++}}$ is seen after the puff, followed by a slow decay which results from the equilibrating He^{++} radial distribution. This density of He^{++} (~ 5% of n_e) is consistent with the observed rise in $\bar{n}_e$. The constant He^+ edge radiation at late times indicates full recycling of helium at the plasma periphery.

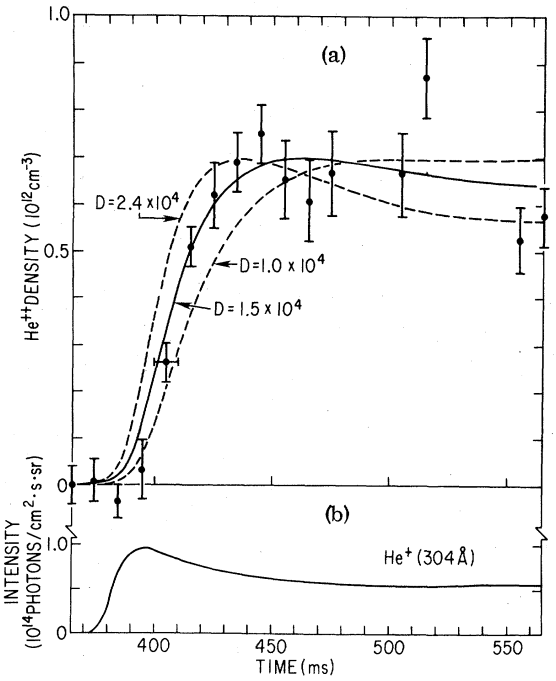

FIG. 2. Change in $n_{He^{++}}(r = 7$ cm) and central-chord He^+ 304-Å radiation after a short helium puff. The solid line is the estimated best fit to the data using the diffusive/convective model discussed in the text, and the dashed curves show the sensitivity of the model to variation of the diffusion coefficient. The peaking factor $c_v = 0.8$ and $c_s = 1.0$ for these curves.

Figure 3 shows the radial profile of He^{++} measured at $t = 550$ ms. The data points are weighted averages of values from both $R \geq R_{pl}$ and $R < R_{pl}$. The absolute scale on this plot is accurate to ~ 30% when spectrometer calibration, beam attenuation, and excitation rate uncertainties are taken into account, but the uncertainty in the relative profile shape is much smaller, being determined mainly by the signal-to-noise ratio attained in a given shot. The data in Fig. 3 also include a correction of ~ 30% for light emitted by electron excitation of He^+ ions which are created along the beam path and drift along the magnetic field lines into the spectrometer line of sight.[15] This correction has only a minor influence on the derived He^{++} radial profile shape.

Cross-field transport coefficients for He^{++} are obtained by modeling the data in Figs. 2 and 3 with solutions of the one-dimensional continuity equations for the helium ions:

$$\frac{\partial}{\partial t} n_q + \frac{1}{r}\frac{\partial}{\partial r}(r\Gamma_q) = -(I_q + R_q)n_q + I_{q-1}n_{q-1} + R_{q+1}n_{q+1} - \frac{n_q}{\tau_\parallel} + S_q. \quad (1)$$

Here, q is the ion charge, n_q is the density of charge state q, Γ_q is the radial flux for charge state q, R_q is the total recombination rate, I_q is the total ionization rate, $\tau_\parallel^{-1}$ denotes an effective loss rate for particles outside the limiter radius (i.e., $\tau_\parallel^{-1} = 0$ for $r < a$), and S_q is a volume source for $q = +1$ resulting from edge neutral influx. All of the terms in Eq. (1) are functions of r, and the coupled equations are solved numerically using the Princeton Plasma Physics Laboratory MIST impurity transport code.[16]

A three-dimensional neutral deposition calculation is used to model a low-energy He^0 influx at the plasma edge which is programmed to reproduce accurately the He^+ (304 Å) time evolution in Fig. 2(b). A multiplicative scale factor was applied to the data in Fig. 2(b) in order to match the observed central He^{++} absolute density. Depending on the transport coefficients used, this factor ranged from 1.6 to 3.2. This is consistent with toroidal asymmetries of H_α emission in PDX discharges. Neutral helium at $E_0 \sim 0.1$ eV arising from desorption from the carbon limiter at $r = a$ is taken as the nominal particle source in our calculations. The exact energy distribution of the recycling He^0 is a function of incident ion energy,[17] surface physics, etc., and is not well known. More energetic He^0 will yield deeper plasma penetration ($r \sim 31$ cm for $E_0 \sim 10$ eV versus $r \sim 38$ cm for $E_0 \sim 0.1$ eV). However, variation of E_0 over this range does not affect our

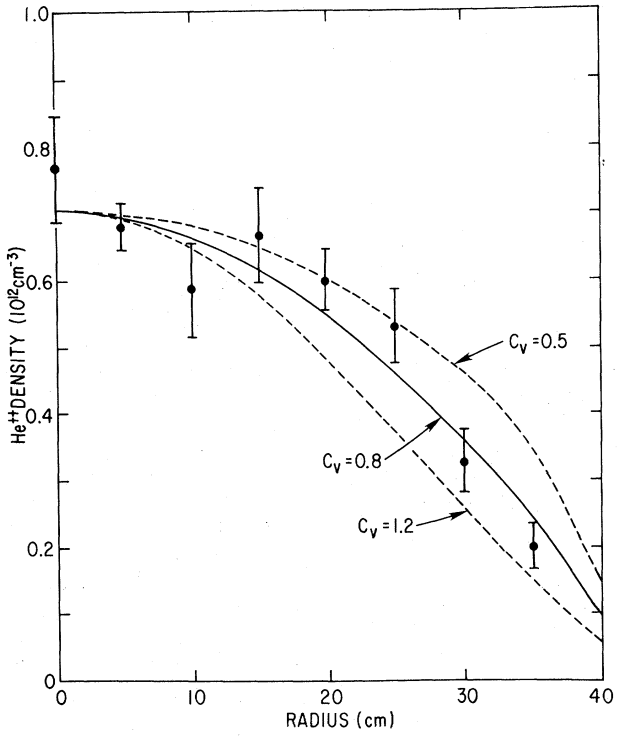

FIG. 3. Radial profile of He^{++} at $t=550$ ms. The solid line is the estimated best fit to the data using the diffusive/convective transport model, while the dashed curves show the sensitivity to variation of the peaking parameter c_v.

transport conclusions to within the accuracy of the present data.

The particular virtue in using He^{++} for particle transport measurements lies in the fact that time and space variations of $n_{He^{++}}$ are predominantly determined by the transport processes of interest instead of the atomic processes on the right side of Eq. (1).

Even a cursory estimate of the values of $\Gamma_{He^{++}}$ needed to reproduce these measurements shows that the required flux is one to two orders of magnitude larger than that expected from neoclassical transport theory, and we thus employ a general diffusive/convective model for the flux to obtain empirical transport coefficients via

$$\Gamma_q(r,t) = -D(r)\frac{\partial n_q(r,t)}{\partial r} + v(r)n_q(r,t), \qquad (2)$$

where the diffusion coefficient $D(r)$ and convective velocity $v(r)$ are both assumed to be independent of time and charge state. This model has been used in transport studies of low- and high-Z impurities[6,9,11,16] and for studies of the plasma density buildup in tokamaks.[18]

In transport equilibrium, the total ionic flux, $\sum\Gamma_q$, is zero in the central, source/sink free region of the plasma. Since $n_{He^{++}}(r) \gg n_{He^{+}}(r)$ in this region as well, the equilibrium radial profile of He^{++} is directly related to the convective and diffusive transport via $v(r)/D(r) = [\partial(\ln n_{He^{++}})/\partial r]$. Noting that the $n_{He^{++}}(r)$ profile is similar to that of $n_e(r)$, we choose the parametrization

$$v(r)/D(r) = c_v\,\partial(\ln n_e)/\partial r, \qquad (3)$$

for all r. In the fully ionized, source-free region, this yields $n_{He^{++}}(r) \propto [n_e(r)]^{c_v}$. If we choose c_v to give the best fit of the entire measured radial profile to profiles calculated via Eq. (1), $D(r)$ can then be derived from knowledge of the time evolution $n_{He^{++}}(t)$ at several radii. Since $n_{He^{++}}(t)$ was measured only at $r=7$ cm in these initial experiments, we parametrize the diffusive transport using a radially constant diffusion coefficient $D(r)=D$.

Fitting of the data of Figs. 2 and 3 with time-evolving solutions to Eq. (1) reveals the calculated radial profiles to be indeed indistinguishably close to equilibrium at $t=550$ ms. Figure 3 shows three such profiles in comparison with the data. The calculated profiles are all normalized to agree with the weighted average of the two innermost data points. The adopted value of $c_v = 0.8 \pm 0.3$ describes a helium radial profile which is similar to $n_e(r)$, but slightly less peaked. Values of c_v toward the lower end of this range are favored as one approaches $E_0 \sim 10$ eV. This result is independent of the assumed value of D, and unambiguously demonstrates the need for a convective term in addition to diffusion in impurity flow models.

Taking $c_v = 0.8$ and modeling the time evolution of the near-central He^{++} in Fig. 2 provides the diffusion coefficient, D. The value of D thus derived is somewhat sensitive to the assumed value of $\tau_{\parallel}$, the effective edge plasma confinement time due to parallel flow to the limiter in the region 40 cm $< r \leq$ 50 cm. In our model, we take $\tau_{\parallel}^{-1} = c_s v_s/\pi q(a) R_{pl}$ where v_s is the plasma sound speed in the scrapeoff, c_s is an adjustable Mach number for parallel flow, and $q(a)$ is the discharge safety factor. In general, if c_s is reduced, a correspondingly higher D is derived from the data. For example, taking $c_s = 1.0$, we arrive at $D = (1.8 \pm 0.6) \times 10^4$ cm^2/s, while $c_s = 0.1$ yields $D = (2.4 \pm 0.6) \times 10^4$ cm^2/s. Representative calculations using $c_s = 1.0$ are shown in Fig. 2 to indicate the sensitivity of the model to variations in D. Taking $0 \leq c_s \leq 1$ together with $c_v = 0.8 \pm 0.3$

yields $D = (2.1 \pm 0.9) \times 10^4$ cm^2 s^{-1}. This error range could be substantially reduced by obtaining $n_{He^{++}}(t)$ time evolution data at several radial points. Such data would also allow the radial dependence of D to be determined.

The enthusiastic support and guidance of D. Post during the course of this work is gratefully acknowledged. We also wish to thank R. Kaita for kindly operating the diagnostic neutral beam, and H. Towner, R. Goldston, C. Singer, K. Bol, and the PDX operating crew for assistance in these studies.

This work was supported by the U. S. Department of Energy under Contract No. DE-AC02-76-CHO-3073.

[1]D. E. Pst, D. R. Mikkelsen, R. A. Hulse, L. D. Stewart, and J. C. Weisheit, J. Fusion Energy 1, 129 (1981).

[2]M. Shimada *et al.*, Phys. Rev. Lett. 47, 796 (1981); J. C. DeBoo, N. H. Brooks, J. S. Degrassie, M. A. Mahdavi, N. Ohyabu, and J. C. Wesley, Nucl. Fusion 22, 572 (1982).

[3]R. E. Chrien, H. P. Eubank, D. M. Meade, and J. D. Strachan, Nucl. Fusion 21, 1661 (1981).

[4]F. Englemann and A. Nocentini, Comments Plasma Phys. Controlled Fusion 5, 261 (1980).

[5]K. H. Burrell, Bull. Am. Phys. Soc. 24, 767 (1979).

[6]E. S. Marmar, J. E. Rice, J. L. Terry, and F. H. Seguin, Nucl. Fusion 22, 1567 (1982).

[7]R. C. Isler *et al.*, Nucl. Fusion 23, 1017 (1983).

[8]K. H. Burrell, S. K. Wong, C. H. Muller, M. P. Hacker, H. Ketterer, R. C. Isler, and E. A. Lazarus, Nucl. Fusion 21, 1009 (1981).

[9]TFR Group, Nucl. Fusion 23, 559 (1983).

[10]R. A. Hulse, Bull. Am. Phys. Soc. 28, 929 (1983).

[11]R. J. Fonck, M. Finkenthal, R. J. Goldston, D. L. Herndon, R. A. Hulse, R. Kaita, and D. D. Meyerhofer, Phys. Rev. Lett. 49, 737 (1982).

[12]A. N. Zimov'ev, A. A. Korotko, E. R. Krzhizhanovskii, V. V. Afrosimov, and Yu. S. Gordeev, Pis'ma Zh. Eksp. Teor. Fiz. 32, 557 (1980) [JETP Lett. 32, 539 (1980)].

[13]R. C. Isler, L. E. Murray, S. Kasai, J. L. Dunlap, S. C. Bates, P. H. Edmonds, E. A. Lazarus, C. H. Ma, and M. Murakami, Phys. Rev. A 24, 2701 (1981).

[14]R. J. Fonck, R. J. Goldston, R. Kaita, and D. E. Post, Appl. Phys. Lett. 42, 239 (1983).

[15]R. J. Fonck, D. S. Darrow, and K. P. Jaehnig, Princeton Plasma Physics Laboratory Report No. PPPL-2067 (to be published).

[16]R. A. Hulse, Nucl. Technol. Fusion 3, 259 (1983).

[17]W. Eckstein and H. Verbeek, Institut für Plasmaphysik Report No. IPP-9/32, 1979 (unpublished).

[18]J. D. Strachan *et al.*, Nucl. Fusion 22, 1145 (1982).